Check for updates

Geophysical Research Letters

RESEARCH LETTER
10.1029/2023GL102959

Contrasting Responses of Atlantic and Pacific Tropical Cyclone Activity to Atlantic Multidecadal Variability

Huanping Huang[1,2], William D. Collins[2,3], Christina M. Patricola[2,4], Yohan Ruprich-Robert[5], Paul A. Ullrich[6,7], and Alexander J. Baker[8]

[1]Department of Geography and Anthropology, Louisiana State University, Baton Rouge, LA, USA, [2]Climate and Ecosystem Sciences Division, Lawrence Berkeley National Laboratory, Berkeley, CA, USA, [3]Department of Earth and Planetary Science, University of California, Berkeley, Berkeley, CA, USA, [4]Department of Geological and Atmospheric Sciences, Iowa State University, Ames, IA, USA, [5]Barcelona Supercomputing Center, Barcelona, Spain, [6]Department of Land, Air and Water Resources, University of California, Davis, CA, USA, [7]Plant and Life Science Directorate, Lawrence Livermore National Laboratory, Livermore, CA, USA, [8]National Centre for Atmospheric Science and Department of Meteorology, University of Reading, Reading, Berkshire, UK

Key Points:

- The warm phase of the Atlantic Multidecadal Variability (AMV) increases tropical cyclone (TC) frequency over the North Atlantic
- By contrast, the warm phase of AMV reduces TC occurrence in the western North Pacific and South Pacific
- The contrast in basinwide TCs is due to opposite changes in thermodynamics and dynamics with warm AMV

Supporting Information:

Supporting Information may be found in the online version of this article.

Correspondence to:

H. Huang,
hhuang@lsu.edu

Citation:

Huang, H., Collins, W. D., Patricola, C. M., Ruprich-Robert, Y., Ullrich, P. A., & Baker, A. J. (2023). Contrasting responses of Atlantic and Pacific tropical cyclone activity to Atlantic Multidecadal Variability. *Geophysical Research Letters*, *50*, e2023GL102959. https://doi.org/10.1029/2023GL102959

Received 27 JAN 2023
Accepted 24 APR 2023

© 2023 Lawrence Berkeley National Laboratory and The Authors.
This is an open access article under the terms of the Creative Commons Attribution-NonCommercial License, which permits use, distribution and reproduction in any medium, provided the original work is properly cited and is not used for commercial purposes.

Abstract This research assesses the influences of Atlantic Multidecadal Variability (AMV) on global tropical cyclones (TCs) using two large ensembles of idealized global climate model simulations with opposite signs of AMV forcings superimposed (i.e., AMV+ and AMV–). We first detect TCs and then compare TC activity by basin in the two AMV experiments. We find contrasting responses of Atlantic and Pacific TC frequency to the AMV anomalies. Compared to AMV–, AMV+ significantly increases TC frequency in the North Atlantic, including those making landfalls. The increase is explained by warmer sea surface temperature, higher relative humidity, increased relative vorticity, and weaker vertical wind shear under AMV+. By contrast, AMV+ decreases TC occurrence over the western North Pacific and South Pacific, which is tied to stronger vertical wind shear and lower relative humidity. The opposite responses of TC activity to AMV+ are attributed to strengthened Walker Circulation between the Atlantic and Pacific.

Plain Language Summary The Atlantic Multidecadal Variability (AMV), a multidecadal variation in North Atlantic sea surface temperatures (SSTs), is a useful predictor for North Atlantic tropical cyclones (TCs). Yet how AMV influences TC activity on a global scale remains poorly understood. To fill this gap, we analyze two sets of idealized climate model simulations which differ from each other by either adding or subtracting AMV anomalies from the mean SST conditions over the North Atlantic. We first identify TCs in the simulations, and then compare and explain their differences. Relative to cold SST anomaly of AMV (AMV–), warm SST anomaly of AMV (AMV+) produces much more frequent TCs (including those making landfalls) over the North Atlantic. This is because AMV+ offers favorable conditions for TC development, including warmer SSTs, higher relative humidity, increased relative vorticity, and weaker vertical wind shear. By contrast, AMV+ causes less frequent TCs across the western North Pacific and South Pacific due to unfavorable conditions for TC occurrence (stronger vertical wind shear and less moist air). The contrasts in TC environment are due to increased zonal flow between the Atlantic and Pacific basins with AMV+.

1. Introduction

Observational evidence has shown a multidecadal variation in Atlantic tropical cyclone (TC) activity and landfalling hurricanes (Chylek & Lesins, 2008; Goldenberg et al., 2001; Klotzbach & Gray, 2008; Knutson et al., 2007; Vecchi & Knutson, 2008). The variation has been tied to the Atlantic Multidecadal Variability (AMV; Chylek & Lesins, 2008; Goldenberg et al., 2001; Vecchi & Knutson, 2008), a climate mode representing sea surface temperature (SST) anomalies over the North Atlantic with a period of approximately 65–80 years (Enfield et al., 2001). Klotzbach et al. (2018) found that over the period 1900–2017, the number of landfalling hurricanes in the US was significantly higher (+27%) during an AMV warm phase than that during an AMV cold phase. As such, the AMV–TC linkage provides an important source of multidecadal predictability of TC activity, leading to the widespread use of AMV in TC predictions (K. Davis et al., 2015; K. Davis & Zeng, 2019; Elsner & Jagger, 2006; Landsea et al., 1999). Furthermore, Klotzbach et al. (2018) reported that median damage from these hurricanes was $6.1 and 0.7 billion, respectively, representing 8.7 times higher economic costs in an AMV warm phase compared to an AMV cold phase. Rappaport and Blanchard (2016) discovered that a majority of the deadliest

hurricanes from 1963 to 2012 occurred during the last two decades. This period coincided with the current AMV warm phase and the rapid increase of population in coastline counties (U.S. Census Bureau, 2021). Given the distinct frequency and impacts of TCs by AMV phase, it is imperative to understand the effects of AMV on TCs and then improve TC predictions.

Numerous studies have found a significant modulation of AMV on basinwide and landfalling TCs in the North Atlantic (NA) (Goldenberg et al., 2001; Klotzbach et al., 2018; Klotzbach & Gray, 2008; Landsea et al., 1999; Ting et al., 2015). Wang et al. (2008) found that AMV was associated with a multidecadal variation in the Atlantic Warm Pool. A large Atlantic Warm Pool, a prominent feature during the warm phase of AMV, may enhance Atlantic TC activity by decreasing vertical wind shear over the hurricane main development region and increasing convective instability. Because large Atlantic Warm Pool induced cyclonic (anticyclonic) circulation anomalies in the lower (upper) troposphere, weakening easterly (westerly) winds and vertical wind shear. By contrast, a small Atlantic Warm Pool, a notable feature during the cold phase of AMV, induced opposite changes, that is, increased vertical wind shear, decreased convective instability, and suppressed Atlantic TC activity. Ting et al. (2015) discovered that recent increases in NA hurricane potential intensity was dominated by the warm phase of AMV since the mid-1990s. Emanuel (2007) reported that three TC environmental factors (potential intensity, vorticity in lower troposphere, and vertical wind shear) varied together with Atlantic sea surface temperatures (SSTs). More notable is that past studies were primarily based on observations and historical simulations, so they cannot clearly separate the effect of AMV on NA TCs from other factors including internal climate variability and anthropogenic climate change. Idealized model simulations only involving AMV differences is therefore needed to quantify the individual effect of AMV on TCs, which is the first novelty of the current study.

AMV has a remote effect on TC activity beyond the Atlantic basin, most notably over the western North Pacific (WP) and the eastern North Pacific (EP). Zhang et al. (2018) concluded that since the mid-1990s, the AMV warm phase had played a much more significant role in reducing WP TC frequency than anthropogenic forcing and the Pacific Decadal Oscillation (PDO). AMV-related warming was the primary driver of observed changes in the Walker circulation, which further led to increased vertical wind shear and decreased TC genesis over the southeastern part of the WP. Similarly, Chan and Liu (2022) discovered a contrast in TC count between the NA and WP since the mid-1990s, which was associated with AMV, the Interdecadal Pacific Oscillation, and the El Niño–Southern Oscillation (ENSO). Wang and Lee (2009) demonstrated an out-of-phase relationship between TC activity in the tropical NA and EP. On multidecadal timescales, the warm phase of AMV was linked to active TCs in the tropical NA and inactive TCs over the EP. The opposite activity pattern was present during the cold phase of AMV. The relationship was primarily associated with vertical wind shear and convective instability, while relative humidity and vorticity variations played a minimal role. Similarly, there is a significant negative correlation between observed TC activity in the North Pacific and the interannual Atlantic Meridional Mode, as well as a significant positive correlation between ENSO and North Pacific TC activity (Patricola et al., 2022). Despite the regional studies identifying a negative correlation between AMV and North Pacific TC frequency, assessing the influence of AMV on TCs on a global scale is still lacking and serves as the second novelty of the current study. What's more, most of these studies (except Zhang et al., 2018) only analyzed observational records, limiting their capability in separating the individual effect of AMV on North Pacific TCs. As discussed earlier, the AMV-focused idealized model simulations in the current study can address the question on whether the abovementioned AMV–North Pacific TC connection is robust or not.

The objective of the current study is to evaluate the individual effects of AMV on TC characteristics on a global scale, including frequency, intensity, latitude and longitude of lifetime maximum intensity, duration, and translation speed. Specifically, we tackle two questions: (a) What are the impacts of different AMV phases on TC activity in each ocean basin? (b) How does AMV affect the oceanic and atmospheric environment in which TCs originate? We used two large ensembles of idealized global climate model (GCM) simulations to address the questions. These ensembles are forced by opposite signs of AMV anomalies (i.e., AMV+ and AMV–) over the NA. By comparing TC activity and large-scale environment in the two AMV experiments, we quantified local and remote controls of AMV on TCs in each basin. The outcome may shed light on one source of multidecadal predictability of worldwide TCs, as well as TC prediction with climate modes on decadal and interannual scales (e.g., PDO and ENSO).

19448007, 2023, 10, Downloaded from https://agupubs.onlinelibrary.wiley.com/doi/10.1029/2023GL102959 by University Of East Anglia, Wiley Online Library on [20/07/2026]. See the Terms and Conditions (https://onlinelibrary.wiley.com/terms-and-conditions) on Wiley Online Library for rules of use; OA articles are governed by the applicable Creative Commons License

19448007, 2023, 10, Downloaded from https://agupubs.onlinelibrary.wiley.com/doi/10.1029/2023GL102959 by University Of East Anglia, Wiley Online Library on [20/07/2026]. See the Terms and Conditions (https://onlinelibrary.wiley.com/terms-and-conditions) on Wiley Online Library for rules of use; OA articles are governed by the applicable Creative Commons License

2. Data and Methods

2.1. Climate Model Simulations

The GCMs used in this study are fully coupled EC-Earth3P-HR and EC-Earth3P (Haarsma et al., 2020) and Centre National de Recherches Météorologiques (CNRM)-CM6-1 (Voldoire et al., 2019), with their characteristics summarized in Table S1 in Supporting Information S1. The climate simulations followed a modified version of the component C—idealized AMV experiments—protocol of the CMIP6 Decadal Climate Prediction Project (DCPP; Boer et al., 2016), and were performed as part of the PRIMAVERA project (Hodson et al., 2022; Ruprich-Robert et al., 2021). The experiments are designed to answer the following questions: What are the effects of AMV on global and regional climate variations? How sensitive are the effects to model resolution & GCM? In the idealized AMV experiments, NA SSTs are restored by superimposing observed AMV anomaly patterns (positive: AMV+, negative: AMV−) on modeled SST climatology (Boer et al., 2016). First, the 12-month SST climatology is derived from the CMIP6 Diagnostic, Evaluation, and Characterization of Klima control simulation integrated with constant external forcing conditions (Eyring et al., 2016). Next, over the restoring region (NA), the AMV forcings are imposed by altering surface fluxes (recommended over restoring SST directly), with a restoring coefficient of 40 W m^{-2} K^{-1} applied (i.e., a 2-month damping timescale for an ocean mixed layer of 50 m). Outside the restoring region, the GCMs are free to evolve, which enables the climate system to fully respond to the AMV forcings (Boer et al., 2016). Here the AMV anomaly patterns were estimated from regressing residual observed SSTs (i.e., forced component subtracted from raw SSTs) on the AMV time series over the period 1900–2013. Technical details on computing the AMV anomaly and restoring NA SST are described in technical notes 1 (https://www.wcrp-climate.org/wgsip/documents/Tech-Note-1.pdf) and 2 (https://www.wcrp-climate.org/wgsip/documents/Tech-Note-2.pdf) for DCPP-Component C. Comparing the AMV+ and AMV− experiments allows us to quantify the effect of AMV on global and basinwide TC activity.

The imposed AMV anomaly in the GCM simulations was 2 standard deviations of the observed AMV (i.e., 2 × AMV), rather than 1 or 3 standard deviations used by other DCPP models (Ruprich-Robert et al., 2021). This selection represents a trade-off between reducing ensemble size needed for detectablesignals and avoiding the exacerbation of AMV impacts. It's also worth noting that it is computationally expensive to generate the large ensemble high-resolution simulations (Hodson et al., 2022). External forcings in the GCM simulations were held constant in the year 1950 level (Ruprich-Robert et al., 2021). The model outputs archived at 6-hourly include sea level pressure, zonal and meridional wind, and air temperature at different vertical levels, which are necessary for TC tracking (see Section 2.2). We note that similar idealized AMV experiments with other GCMs were conducted in the DCPP and PRIMAVERA projects. But the temporal frequency of their model outputs is generally monthly and/or daily, which is not enough for TC tracking at high frequency (6-hourly and finer). Among the three GCMs used in the current study, only the EC-Earth3P-HR model was run at a high resolution (~50 km), while the EC-Earth3P (~100 km) and CNRM-CM6-1 (~200 km) simulations were performed at coarse resolutions. Recent studies demonstrate the importance of using high-resolution models to simulate TCs (Roberts et al., 2020a, 2020b). Therefore, we focus on the results derived from the EC-Earth3P-HR model in the main text and present results from the two low-resolution GCMs in Supporting Information S1. As described in Table S1 in Supporting Information S1, the EC-Earth3P-HR ensemble we analyzed consists of 10 ensemble members generated from macro-perturbations, and each ensemble simulation spans a 10-year period. Past studies show that historical simulations with the EC-Earth3P-HR model generally reproduce the spatial patterns of TCs over the globe, with the most active TCs in the WP (Roberts et al., 2020a). Yet the GCM underestimates TC count and intensity (Kreussler et al., 2021; Roberts et al., 2020a, 2020b). For example, Roberts et al. (2020b) concluded that the coupled EC-Earth3P-HR model simulates 58.7% less TCs globally compared to observations, but the model reasonably captures relative frequency of TCs by basin (percentage of global total).

2.2. Tropical Cyclone Tracking

To identify TC tracks and their lifecycle in the model outputs, we first leveraged a feature-tracking algorithm named TempestExtremes (Ullrich et al., 2021). TempestExtremes uses sea level pressure as its primary feature-tracking variable, with additional constraints from air temperature, wind speed, and other environmental variables at 6-hourly resolution. Compared to other tracking algorithms, TempestExtremes requires less but well-known variables as inputs (Bourdin et al., 2022), making TC detection with the GCM outputs possible. We used the following procedures to track TCs. First, we detected TC candidates by finding local minima in sea level

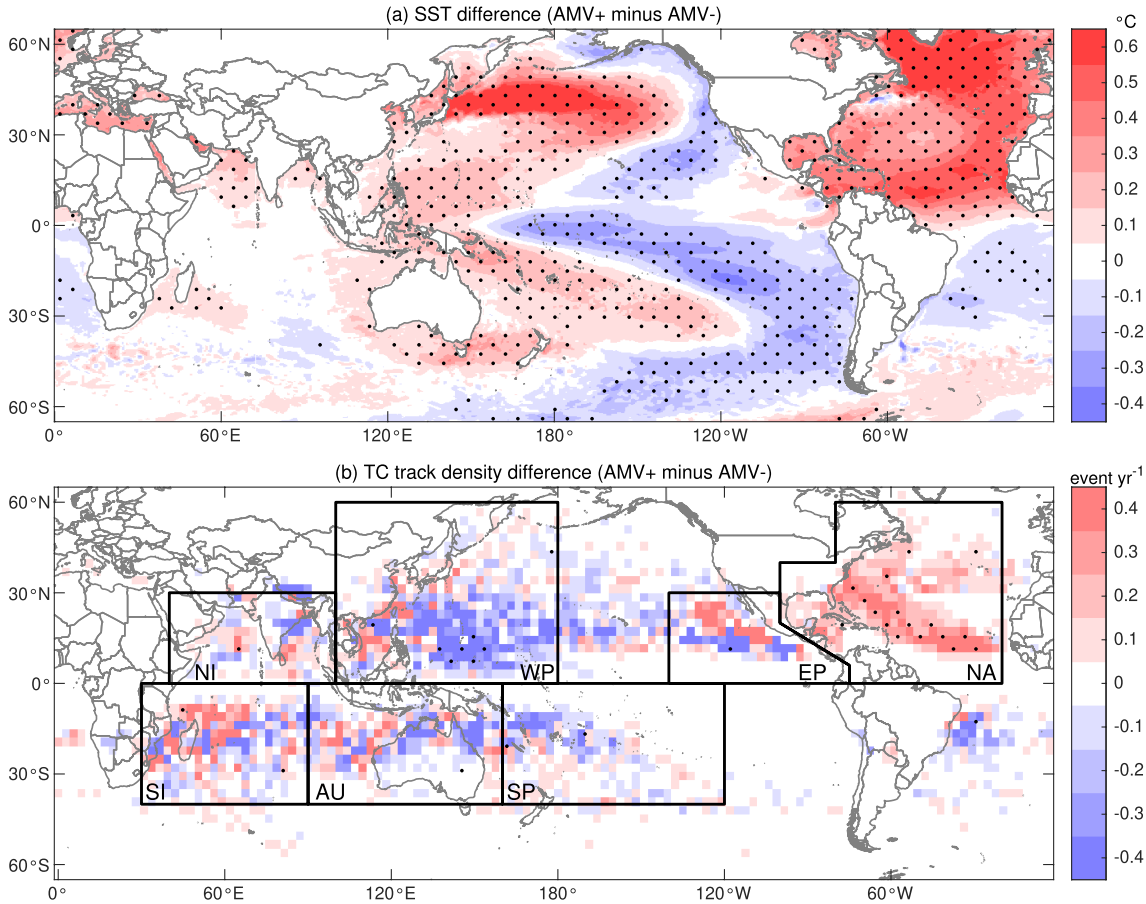

Figure 1. Differences in ensemble-averaged (a) sea surface temperature and (b) tropical cyclone (TC) track density between the AMV+ and AMV− experiments performed with the EC-Earth3P-HR model. TC track density in (b) is aggregated over 8 × 8 grid boxes (i.e., approximately 400 × 400 km) to account for low density of TC in each high-resolution grid box. Black boxes in (b) show the seven TC basins analyzed, including North Atlantic, eastern North Pacific, western North Pacific, North Indian, South Indian, Australian, and South Pacific. Stippling indicates a significant difference based on the two-sample *t*-test ($\alpha = 0.05$, $n = 10$). Each sample corresponds to the average of an ensemble member spanning 10 years.

pressure over all 12 months each year. Candidates are eliminated if they do not satisfy a closed contour criterion, which requires that (a) sea level pressure increases by ≥2 hPa over a 5.5° radius of the candidate; and (b) averaged air temperature over 250–500 hPa decreases by ≥0.4°C over a 6.5° radius of the candidate (maximum temperature searched within 1° radius of the candidate). Next, the resultant candidates are connected together in time to form TC tracks. The duration of a TC track has to be ≥54 hr (i.e., 10 six-hourly time steps), with a maximum temporal gap (spatial distance) allowed at 24 hr (8°) between two candidates. In addition, a TC path must meet the following thresholds for at least 54 hr: composite wind speed ≥10 m s^{-1} at 925 hPa, latitude ranging between 40°S and 40°N, and surface geopotential ≤150 m^2 s^{-2}. After deriving TC tracks, we compared TC statistics and large-scale TC environment in the two AMV experiments. We analyzed the response of TCs to AMV by ocean basin, which includes NA, EP, WP, North Indian (NI), South Indian (SI), Australian (AU), and South Pacific (SP), as shown in Figure 1b. The South Atlantic is not included because the GCM does not simulate any TC in this basin.

To assess the sensitivity of TC responses to feature-tracking algorithm, we used a different algorithm named TRACK (K. I. Hodges, 1995, 1999) and compared its results with those derived from the TempestExtremes. The TRACK algorithm was widely applied to track TCs in reanalyzes and GCM outputs (Baker et al., 2021, 2022; K. Hodges et al., 2017; Roberts et al., 2020a, 202b). Different from TempestExtremes, TRACK uses relative vorticity in various vertical levels as the primary feature-tracking variables. It is worth noting that these vertical levels were all available for the CNRM-CM6-1, but not for the EC-Earth3P(-HR) ensemble outputs. Therefore, we only tracked TCs in the CNRM-CM6-1 model outputs with TRACK. More details on the tracking method are described in Text S1 in Supporting Information S1.

19448007, 2023, 10, Downloaded from https://agupubs.onlinelibrary.wiley.com/doi/10.1029/2023GL102959 by University Of East Anglia, Wiley Online Library on [20/07/2026]. See the Terms and Conditions (https://onlinelibrary.wiley.com/terms-and-conditions) on Wiley Online Library for rules of use; OA articles are governed by the applicable Creative Commons License

3. Results and Discussion

3.1. The Influences of AMV on TC Activity

In agreement with the imposed constraints in the EC-Earth3P-HR model, NA SSTs in the AMV+ experiment are significantly warmer than those in the AMV− experiment ($p < 0.05$; Figure 1a). Conversely, SSTs cool slightly over the South Atlantic and more prominently over the off-equatorial eastern Pacific. To the west of the cooling areas, SSTs increase in most of the western Pacific and NI. The spatial contrasts, most notably the Atlantic–Pacific teleconnection, are in agreement with Meehl et al. (2020) and Ruprich-Robert et al. (2021). Li et al. (2015) reported that the responses of tropical Pacific SSTs to AMV forcings are resulted from the wind–evaporation–SST effect and Bjerknes feedback. Specifically, AMV+ and associated Atlantic convection enhance easterly wind and evaporation over the off-equatorial eastern Pacific, leading to cooler SSTs. By contrast, AMV+ weakens westerly wind and evaporation over the NI, which warms up SSTs. The resulting changes in SST gradient produce a secondary Indo–western Pacific convection which strengthens easterly wind and the Ekman pumping in the eastern Pacific. As a result, the altered atmospheric and oceanic circulations further intensify the La Niña-type response (i.e., cooler eastern Pacific and warmer western Pacific) and global SST dipole pattern (Li et al., 2015).

The AMV forcings cause significant changes in TC frequency over the NA and Pacific basins, but induce few changes in other basins. Compared to AMV−, AMV+ significantly increases TC frequency over the tropical and western NA, but decreases TC frequency in the tropical WP basin (Figure 1b). Averaging TC frequency over each basin (Figure S1a in Supporting Information S1), we find that AMV+ produces 3.8 TCs per year in the NA, indicating a 90% increase compared to AMV− (2.0 TCs per year; $p < 0.01$). By contrast, AMV+ leads to 9.3% and 14.7% reductions ($p < 0.05$) in TC frequency across the WP and SP, respectively (see Figure S2 in Supporting Information S1 for individual ensemble members). The contrast between TC frequency in the NA and North Pacific resembles the response of North Pacific TCs to La Niña events (Fu et al., 2019), and aligns with Zhang et al. (2018) and Murakami et al. (2020). Here we further demonstrate the remote effect of AMV on SP TCs. Unlike Wang and Lee (2009), we find that EP TCs are insensitive to the AMV forcings. The intra-basin response of EP TCs, albeit statistically insignificant, resembles the spatial pattern of the TC response to ENSO (Fu et al., 2017). We note that although the flux-corrections were only applied in the NA to mimic AMV, an ENSO-like response in the Pacific also forms. Here we primarily explore the TC responses to the overall SST pattern arising from the AMV forcings, rather than to what extent the TC responses are driven by Atlantic or Pacific SSTs.

For landfalling TCs, we find a significant increase in their frequency (0.3 events yr^{-1}) over the NA basin when comparing AMV+ to AMV− (Figure S1b in Supporting Information S1). Our finding aligns qualitatively with past studies based on observations (Goldenberg et al., 2001; Huang et al., 2018; Klotzbach et al., 2018), as they all showed a significant increase in landfalling TCs during AMV+ conditions. Here we note that the percentage of NA TCs making landfall remains similar during the AMV− and AMV+ phases (16%–17%). In other basins, landfalling TC frequencies in the two AMV experiments are not significantly different.

TC intensity, characterized by the minimum sea level pressure at TC centers, is minimally affected by the AMV anomalies (Figure S1c in Supporting Information S1). A significant change in AMV-induced TC intensity is found over the EP and AU oceans ($p < 0.05$), yet the differences in average intensity between the two AMV experiments are less than 1 hPa. Over the NA, the difference in TC intensity is insignificant ($p = 0.44$). When only considering landfalling TCs, their intensities due to the AMV+ anomalies do not differ from those produced by the AMV− anomalies (Figure S1d in Supporting Information S1). This appears to contradict with Ting et al. (2015) who found increased potential intensity (calculated from SST) of NA TCs with AMV+. However, potential intensity of TC indicates its theoretical upper limit and may not necessarily translate into actual TC intensity given that the EC-Earth3P-HR model and other GCMs usually underestimate TC intensity (Huang, Patricola, & Collins, 2021; Roberts et al., 2020a). It is suggested that grid spacings of GCMs should be finer than 25 km to simulate category 4 and 5 TCs (C. A. Davis, 2018), which are higher than the resolution of the EC-Earth3P-HR simulations (ocean: ∼28 km, atmosphere: ∼50 km). Additionally, the model's deficiency in representing atmosphere-ocean coupling (e.g., large-scale SST bias and local scale TC-ocean feedback) also contributes to the underestimated TC intensity (Huang, Patricola, & Collins, 2021). Therefore, the modulation of AMV on TC intensity warrants further study, especially with GCMs that are run at very high resolutions and adequately capturing atmosphere-ocean coupling. We reiterate that despite the underestimations of TC intensity and count, the GCM reasonably captures

19448007, 2023, 10, Downloaded from https://agupubs.onlinelibrary.wiley.com/doi/10.1029/2023GL102959 by University Of East Anglia, Wiley Online Library on [20/07/2026]. See the Terms and Conditions (https://onlinelibrary.wiley.com/terms-and-conditions) on Wiley Online Library for rules of use; OA articles are governed by the applicable Creative Commons License

19448007, 2023, 10, Downloaded from https://agupubs.onlinelibrary.wiley.com/doi/10.1029/2023GL102959 by University Of East Anglia, Wiley Online Library on [20/07/2026]. See the Terms and Conditions (https://onlinelibrary.wiley.com/terms-and-conditions) on Wiley Online Library for rules of use; OA articles are governed by the applicable Creative Commons License

relative frequency of TCs by basin, raising the confidence in the contrasting response of Atlantic and Pacific TC frequency to AMV.

Besides TC frequency and intensity, we also evaluated the influences of AMV on other TC characteristics, including latitude and longitude of lifetime maximum intensity, duration, and translation speed. Figure S3 in Supporting Information S1 shows that with AMV+, NA TCs significantly last longer (+13%), move slower (−7.1%), and shift the location of their lifetime maximum intensity closer to the equator (−2.2°). Compared to observational evidence, the first two changes are in qualitative agreement with Webster et al. (2005) on longer duration and Kossin (2018) on slower translation speed, suggesting positive contributions of the current AMV warm phase to the observational trends. However, the third change, tied to the spatial pattern of AMV forcing (i.e., higher warming rate over the tropical NA than the subtropical NA; Figure 1a), contradicts with Kossin et al. (2014) who discovered a poleward migration of observed TC maximum intensity. This disagreement implies that non-AMV factors (especially anthropogenic warming) might be critical drivers of the poleward migration. In other basins, these TC characteristics are generally not much different between AMV+ and AMV–.

Are the contrasting responses of TC activity over the NA and Pacific basins sensitive to model resolution, GCM, and TC tracking algorithm? To address this question, we further detected and analyzed TCs in the EC-Earth3P and CNRM-CM6-1 models. The results are shown in Figures S4, S5, and S6 in Supporting Information S1, with their key statistics summarized in Table S2 in Supporting Information S1. The evidence confirms the above-mentioned findings that AMV+ significantly increases TC frequency over the NA, but decreases TC frequency in the WP and SP basins. The magnitudes of frequency change vary by model and tracking algorithm. Over the EP, the qualitative responses of TCs to the AMV forcings depend on GCM and TC tracking algorithm. Outside the NA and Pacific basins, the responses of TC frequency to the AMV forcings are muted. For landfalling TCs, all the three GCMs yield a significant increase in its frequency in the NA basin (Figures S1, S4–S6 in Supporting Information S1), implying a low sensitivity of the AMV–TC connection to model resolution and GCM. In other basins, there are very small differences in landfalling TCs between the two AMV experiments. It is worth noting that with the same CNRM simulations, the TRACK algorithm (based on relative vorticity) detects a much higher percentage of TCs that make landfall as compared to the TempestExtremes algorithm (based on sea level pressure), especially over the NA basin (TRACK: 62%–66%; TempestExtremes: 13%–14%). This is attributed to a higher percentage of TRACK-derived TCs that originate in the Caribbean Sea and cross over to the EP (not shown), consistent with Baker et al. (2022). The higher precentage is largely due to the vorticity-based TRACK being more permissive in its detections, therefore yielding a higher landfall percentage. Detecting extended tracks permits the latter stages of storms to be tracked, including landfall, when storms normally weaken rapidly. However, this can also increase its false alarms compared with relatively truncated best-track data (Bourdin et al., 2022). This highlights the importance of using different TC tracking methodologies to study TC responses and estimate their uncertainties. Consistent with the EC-Earth3P-HR model, both the EC-Earth3P and CNRM-CM6-1 models show negligible differences in TC intensity between the AMV+ and AMV− conditions.

3.2. The Roles of AMV in Altering TC Environment

What physical drivers are responsible for the TC frequency changes due to the AMV forcings? Given that SST anomalies are superimposed over the NA, we first explored the relationship between basinwide TC frequency and tropical SSTs (averaged over 10–20°N or 10–20°S) in the same basin. Figure S2a in Supporting Information S1 shows a clear separation of NA TC frequency by AMV forcing. By average, SSTs over the tropical NA are 27.6 and 27.0°C in the AMV+ and AMV– experiments, respectively. Their corresponding TC frequencies are 3.8 and 2.0 events per year. The AMV–Atlantic TC correlation agrees with Wang et al. (2008) who also found that AMV modulates NA TC activity via affecting SSTs and therefore moist static instability over the hurricane main development region (10–20°N, 20–80°W). Over the tropical WP, AMV+ derived SST is 0.15°C warmer than AMV– derived SSTs ($p < 0.01$), but its TC frequency is 1.4 events per year (9.3%) lower. Over the tropical SP, SSTs are virtually the same in both the AMV+ and AMV– experiments (28.0°C), but TC frequency decreases by 0.6 event per year (14.7%) with AMV+ compared to AMV–. The findings suggest that over the WP and SP, AMV-related SST changes are not the determinant of the TC frequency decreases.

Next we examined another environmental variable critical for TC genesis—vertical wind shear (i.e., difference between 850 and 250 hPa winds), and analyzed how it could be altered by the AMV forcings. Here we focus on

19448007, 2023, 10, Downloaded from https://agupubs.onlinelibrary.wiley.com/doi/10.1029/2023GL102959 by University Of East Anglia, Wiley Online Library on [20/07/2026]. See the Terms and Conditions (https://onlinelibrary.wiley.com/terms-and-conditions) on Wiley Online Library for rules of use; OA articles are governed by the applicable Creative Commons License

the peak TC season, that is, July–October in the Northern Hemisphere and January–April in the Southern Hemisphere. We find that AMV+ significantly decreases vertical wind shear by more than 3 m s^{-1} over the Atlantic hurricane main development region (Figure S7a in Supporting Information S1). The change in vertical wind shear partially explains why NA TCs become more frequent with AMV+ conditions. Combined with warmer SSTs, they altogether create favorable conditions to generate TCs. The evidence is supported by Wang et al. (2008) who discovered a decreased (increased) vertical wind shear with AMV+ (AMV–). Over the extratropical NA and North America, AMV+ causes a slight increase in vertical wind shear, but the magnitude (0.5–1 m s^{-1}) is much weaker than over the tropical NA (Figure S7a in Supporting Information S1). The environment helps maintain the TCs that form over the tropical NA, giving rise to landfalling TCs. As expected, we find comparable increases in TC frequency over the NA basin (90%) and North America continent (106%).

Further to the west, there is a significant increase (decrease) in vertical wind shear under (above) 15°N of the EP (Figure S7a in Supporting Information S1). The spatial contrast corresponds well to the spatial changes in TC track density across the EP (Figure 1b). This implies that vertical wind shear plays a critical role in modulating TC occurrence across this basin. Patricola et al. (2017) also found a teleconnection between the Atlantic Meridional Mode and vertical wind shear over the EP in model experiments and observations. In the southeastern region (160°E–180°) of the WP (Figure S7a in Supporting Information S1), vertical wind shear increases significantly with AMV+, which contributes to the decreased TC frequency. Zhang et al. (2018) discovered a similar increase in vertical wind shear over the same region and further attributed the recent TC decrease over the WP to the current AMV warm phase. Interestingly, the absolute change in vertical wind shear is much smaller than that in the tropical NA. This response, combined with slightly warmer SSTs over the central and WP (Figure 1a), may help explain why basinwide TC frequency in the WP only experiences a small change (−9.3%). Similarly, in the off-equatorial SP (Figure S7b in Supporting Information S1), increased vertical wind shear is tied to decreased TC frequency during AMV+. In the other ocean basins, there are areas experiencing significant changes in vertical wind shear, but they do not translate into TC frequency anomalies due to other environmental factors (discussed below). To sum up, the AMV forcings modulate TC occurrence over the NA and Pacific by altering vertical wind shear.

Besides SSTs and vertical wind shear, we also assessed other large-scale environment that is critical to TC genesis, including relative humidity at the middle troposphere and relative vorticity at the lower troposphere. Relative humidity responds to the AMV+ forcing in a similar way as SSTs, characterized by increased relative humidity over the NA and decreased relative humidity across part of the Pacific mimicking the La Niña-type response (Figure S8 in Supporting Information S1). This indicates that relative humidity may partially explain the TC frequency contrast over the Atlantic and Pacific. For relative vorticity (Figure S9 in Supporting Information S1), its responses to AMV+ are mixed over the NA, but the subregion with increased relative vorticity overlaps with the area with increased TC occurrence. By contrast, relative vorticity doesn't change significantly over most of the WP during July–October and over the SP during January–April. This suggests that relative vorticity is an important driver of the increased TCs in the NA, but it plays a lesser role in modulating TCs over the Pacific. To better diagnose the drivers of the TC frequency decrease over the WP (primarily over its eastern half between 140°E and 180°), we further divided the domain into two sub-basins. In the sub-basin between 140°E and 160°E (Figure 1b stippled area), there are decreased wind shear (small but significant), increased relative vorticity (insignificant), and decreased relative humidity (significant). While the first two factors create favorable conditions for TC development, the last factor produces unfavorable conditions. Thus, the TC frequency decrease in this sub-basin may be primarily caused by decreased relative humidity. In the sub-basin between 160°E and 180°, there exist increased wind shear (significant), decreased relative humidity (significant), and increased relative vorticity (significant). As the first two factors lead to unfavorable conditions for TC development, the last factor favors TCs. As such, the TC frequency decrease over this sub-basin (160°E–180°) may be induced by increased wind shear and decreased relative humidity.

The considerable impacts of vertical wind shear on inter-basin TC activities raise the question about how AMV influences vertical wind shear. To diagnose the linkage, we further investigated how different components of vertical wind shear (i.e., 850 and 250 hPa winds) change with the AMV forcings (Figure 2). In the Northern Hemisphere, the Hadley cell is characterized by northeasterly trade winds in lower troposphere (e.g., 850 hPa) and northerly flow in upper troposphere (e.g., 250 hPa). The patterns still hold regardless of AMV+ or AMV− conditions (not shown), but their wind speeds are altered by AMV, because AMV warming (AMV+) triggers a deeper Atlantic convection and increases outflow in upper troposphere (both relative to AMV–). This further modifies

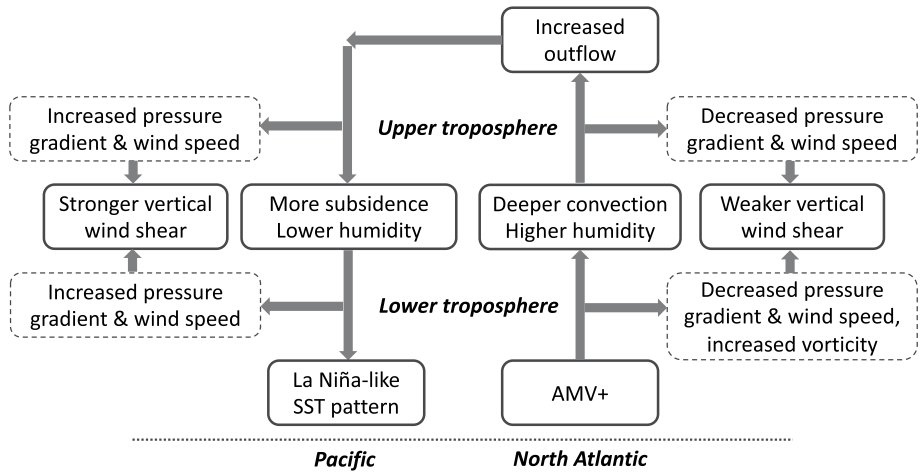

Figure 2. Schematic diagram explaining the AMV+ induced changes that cause the contrasting responses of North Atlantic (NA) and Pacific tropical cyclone frequency. The dashed boxes show the effects of more subsidence (Pacific basin) and deeper convection (NA basin) on the upper (850 hPa) and lower (250 hPa) parts of the troposphere.

the Walker Circulation, enhancing subsidence over the eastern and central Pacific (Figure S10 in Supporting Information S1). The vertical speed divergence must be balanced by horizontal speed divergence due to mass conservation. As a result, the deepened Atlantic convection significantly reduces 850 hPa geopotential height around the Azores High (Figure S11b in Supporting Information S1), which decreases the pressure gradient and therefore wind speed over the tropical NA. At 250 hPa, larger increases in geopotential height over the subtropics (relative to the tropics; Figure S11a in Supporting Information S1) cause similar decreases in pressure gradient and wind speed. The concurrent decreases in both the 850 and 250 hPa winds ultimately produce a weaker vertical wind shear over the tropical NA, as shown in Figure S7a in Supporting Information S1.

Over the North Pacific, however, there exist significant increases in 850 hPa geopotential height around the North Pacific High (Figure S11b in Supporting Information S1), increasing the pressure gradient and thus wind speed. Similarly, 250 hPa geopotential height increases significantly over the central North Pacific except over 15–30°N (Figure S11a in Supporting Information S1). This raises the pressure gradient between the tropics and subtropics centered at 180°, accelerating wind speed. The simultaneous increases in both the 850 and 250 hPa wind speeds (opposite directions) yield a stronger vertical wind shear over the southeastern portion (160°E–180°) of the WP (Figure S7a in Supporting Information S1). In the sub-basin between 140°E and 160°E of the WP, decreased vertical wind shear is mainly due to the increased alignment of 850 hPa winds with 250 hPa winds, which is also a result of the expansion and strengthening of the North Pacific High. However, the abovementioned analysis has revealed that it's relative humidity that reduces TC frequency in the sub-basin, rather than vertical wind shear. To sum up, the strengthened Walker Circulation between the Atlantic and Pacific basins, also revealed by Meehl et al. (2020), links the AMV+ forcing with the altered vertical wind shear as shown in Figure S7 in Supporting Information S1. The pathway aligns with Zhang et al. (2018) who found that the AMV-driven warming since the mid-1990s was the critical driver of increased vertical wind shear and the decreased TC genesis over the southeastern part of WP. In the SP and during its TC peak season (January to April), AMV+ triggers similar increases in pressure gradient and wind speed at both the 850 and 250 hPa levels (not shown), which is also tied to the strengthened Walker Circulation. The regional responses echo the changes that occur over the WP. As noted previously, the strengthened Walker Circulation is also associated with the contrasting changes in SSTs and therefore relative humidity.

4. Conclusions

AMV provides an important source of multidecadal predictability of NA TCs, yet it remains unclear whether or not AMV can serve as a predictor for TC activity on a global scale. To fill this gap, we analyzed two large ensembles of idealized AMV simulations using the same GCM (EC-Earth3P-HR) but with opposite signs of AMV forcings imposed (i.e., AMV+ and AMV–). By comparing TC activity and environment in the two AMV

19448007, 2023, 10, Downloaded from https://agupubs.onlinelibrary.wiley.com/doi/10.1029/2023GL102959 by University Of East Anglia, Wiley Online Library on [20/07/2026]. See the Terms and Conditions (https://onlinelibrary.wiley.com/terms-and-conditions) on Wiley Online Library for rules of use; OA articles are governed by the applicable Creative Commons License

19448007, 2023, 10, Downloaded from https://agupubs.onlinelibrary.wiley.com/doi/10.1029/2023GL102959 by University Of East Anglia, Wiley Online Library on [20/07/2026]. See the Terms and Conditions (https://onlinelibrary.wiley.com/terms-and-conditions) on Wiley Online Library for rules of use; OA articles are governed by the applicable Creative Commons License

experiments, we discover contrasting responses of Atlantic and Pacific TC frequency to the AMV anomalies. Compared to AMV–, AMV+ significantly increases TC frequency in the NA by 90% (1.8 TCs per year) and more than doubles the number of landfalling TCs. The increase is linked to AMV-induced changes in thermodynamics (warmer SSTs and higher relative humidity) and dynamics (weaker vertical wind shear and increased relative vorticity). By contrast, AMV+ decreases TC frequency over the WP and SP by 9.3% and 14.7%, respectively. Both reductions are closely tied to increased vertical wind shear and decreased relative humidity. The contrast between Atlantic and Pacific TC frequency may be explained by the strengthened Walker Circulation between the two basins, which is triggered by the AMV warming (AMV+). Furthermore, the AMV forcings have minor impacts on TC intensity across all basins possibly due to GCMs' limitation in simulating intense TCs. We also investigated the sensitivity of the AMV–TC connections to model resolution, GCM, and TC tracking algorithm, and conclude that the abovementioned AMV–TC connections are robust.

Besides TC frequency and intensity, other TC characteristics (including latitude and longitude of lifetime maximum intensity, duration, and translation speed) and their linkage with AMV were also evaluated. We find that with AMV+, NA TCs significantly last longer (+13%), move slower (−7.1%), and shift the location of their lifetime maximum intensity closer to the equator (−2.2°). In contrast, the TC characteristics in other basins are generally not much different between AMV+ and AMV–.

There are some caveats in the study. First, we make no assumption about the linearity of TC response to different strengths of AMV, and therefore the findings should be interpreted in the context of the 2 × AMV forcing experiments. Future work including different strengths of AMV may help answer whether or not TC activity responds linearly to different strengths of AMV. Second, the sensitivity of the AMV–TC connections to GCM and tracking algorithm is addressed in the study. But we lacked the model data and computing resource to diagnose its sensitivity to model configurations (e.g., physics and parameterization), which needs to be further explored in future work. Third, constrained by the availability of high-frequency climate data, we used three GCMs and two TC trackers to identify TCs. Future projects for GCM intercomparison should be better coordinated to retain model outputs, facilitating the use of more GCMs to assess TC uncertainties. Finally, the origin of AMV, either being a natural mode or arising from natural and anthropogenic forcings, remains hotly debated (see overview by Huang, Patricola, Winter, et al., 2021). Future improvements in simulating TCs and applying the SST-restoring (Huang, Patricola, & Collins, 2021; O'reilly et al., 2022) will also help us better understand the modulation of AMV on TCs.

Data Availability Statement

- The DCPP climate model outputs at daily and monthly timescales can be accessed through the Earth System Grid Federation nodes (https://esgf-index1.ceda.ac.uk/search/cmip6-ceda).
- Subdaily outputs from the EC-Earth3P-HR, EC-Earth3P, and CNRM-CM6-1 simulations can be accessed at the UK Centre for Environmental Data Analysis's JASMIN platform (https://www.ceda.ac.uk/services/jasmin/).
- The tropical cyclone tracks derived from the EC-Earth3P-HR, EC-Earth3P, and CNRM-CM6-1 simulations are archived at the NERSC portal (https://portal.nersc.gov/archive/home/projects/cascade/www/TC_tracks_AMV).

Acknowledgments
This material is based upon work supported by the U.S. Department of Energy, Office of Science, Office of Biological and Environmental Research, Climate and Environmental Sciences Division, Regional & Global Model Analysis Program, under Award Number DE-AC02-05CH11231. CMP acknowledges support from the U.S. Department of Energy, Office of Science, Office of Biological and Environmental Research (BER), Earth and Environmental Systems Modeling (EESM) Program, under Early Career Research Program Award Number DE-SC0021109. YRR received the support of a fellowship from "la Caixa" Foundation (ID 100010434) and from the European Union's Horizon 2020 research and innovation programme under the Marie Skłodowska-Curie grant agreement No 847648. The fellowship code is LCF/BQ/PR21/11840016. AJB was supported by the PRIMAVERA project (European Commission Horizon 2020 Grant Agreement 641727) and a National Environmental Research Council national capability grant: The North Atlantic Climate System: Integrated Study (ACSIS) (Grants NE/N018001/1, NE/N018044/1, NE/N018028/1, and NE/N018052/1). This research used resources of the National Energy Research Scientific Computing Center (NERSC), a U.S. Department of Energy Office of Science user Facility operated under Contract No. DE-AC02-05CH11231. This manuscript is also part of the IS-ENES3 project that has received funding from the European Union's Horizon 2020 research and innovation programme under grant agreement No. 824084. The authors greatly appreciate Malcolm Roberts and Jon Seddon (UK Met Office Hadley Centre) for their help in accessing the model data through the UK Centre for Environmental Data Analysis's JASMIN platform. We acknowledge the World Climate Research Programme, which, through its Working Group on Coupled Modelling, coordinated and promoted CMIP6. We thank the climate modeling groups for producing and making available their model output, the Earth System Grid Federation (ESGF) for archiving the data and providing access, and the multiple funding agencies who support CMIP6 and ESGF.

References

Baker, A. J., Hodges, K. I., Schiemann, R. K. H., & Vidale, P. L. (2021). Historical variability and lifecycles of North Atlantic midlatitude cyclones originating in the tropics. *Journal of Geophysical Research: Atmospheres*, *126*(9), e2020JD033924. https://doi.org/10.1029/2020JD033924

Baker, A. J., Roberts, M. J., Vidale, P. L., Hodges, K. I., Seddon, J., Vannière, B., et al. (2022). Extratropical transition of tropical cyclones in a multiresolution ensemble of atmosphere-only and fully coupled global climate models. *Journal of Climate*, *35*(16), 5283–5306. https://doi.org/10.1175/JCLI-D-21-0801.1

Boer, G. J., Smith, D. M., Cassou, C., Doblas-Reyes, F., Danabasoglu, G., Kirtman, B., et al. (2016). The decadal climate prediction project (DCPP) contribution to CMIP6. *Geoscientific Model Development*, *9*(10), 3751–3777. https://doi.org/10.5194/GMD-9-3751-2016

Bourdin, S., Fromang, S., Dulac, W., Cattiaux, J., & Chauvin, F. (2022). Intercomparison of four tropical cyclones detection algorithms on ERA5. Retrieved from https://egusphere.copernicus.org/preprints/2022/egusphere-2022-179/

Chan, J. C. L., & Liu, K. S. (2022). Recent decrease in the difference in tropical cyclone occurrence between the Atlantic and the western North Pacific. *Advances in Atmospheric Sciences*, *39*(9), 1387–1397. https://doi.org/10.1007/S00376-022-1309-X

Chylek, P., & Lesins, G. (2008). Multidecadal variability of Atlantic hurricane activity: 1851–2007. *Journal of Geophysical Research*, *113*(D22), D22106. https://doi.org/10.1029/2008JD010036

Davis, C. A. (2018). Resolving tropical cyclone intensity in models. *Geophysical Research Letters*, *45*(4), 2082–2087. https://doi.org/10.1002/2017GL076966

Davis, K., & Zeng, X. (2019). Seasonal prediction of North Atlantic accumulated cyclone energy and major hurricane activity. *Weather and Forecasting*, *34*(1), 221–232. https://doi.org/10.1175/WAF-D-18-0125.1

Davis, K., Zeng, X., & Ritchie, E. A. (2015). A new statistical model for predicting seasonal North Atlantic Hurricane activity. *Weather and Forecasting*, *30*(3), 730–741. https://doi.org/10.1175/WAF-D-14-00156.1

Elsner, J. B., & Jagger, T. H. (2006). Prediction models for annual U.S. hurricane counts. *Journal of Climate*, *19*(12), 2935–2952. https://doi.org/10.1175/JCLI3729.1

Emanuel, K. (2007). Environmental factors affecting tropical cyclone power dissipation. *Journal of Climate*, *20*(22), 5497–5509. https://doi.org/10.1175/2007JCLI1571.1

Enfield, D. B., Mestas-Nunez, A. M., & Trimble, P. J. (2001). The Atlantic Multidecadal Oscillation and its relationship to rainfall and river flows in the continental U.S. *Geophysical Research Letters*, *25*(10), 2077–2080. https://doi.org/10.1029/2000GL012745

Eyring, V., Bony, S., Meehl, G. A., Senior, C. A., Stevens, B., Stouffer, R. J., & Taylor, K. E. (2016). Overview of the Coupled Model Intercomparison Project Phase 6 (CMIP6) experimental design and organization. *Geoscientific Model Development*, *9*(5), 1937–1958. https://doi.org/10.5194/gmd-9-1937-2016

Fu, D., Chang, P., & Patricola, C. M. (2017). Intrabasin variability of East Pacific tropical cyclones during ENSO regulated by central American gap winds. *Scientific Reports*, *7*(1), 1–8. https://doi.org/10.1038/s41598-017-01962-3

Fu, D., Chang, P., Patricola, C. M., & Saravanan, R. (2019). High-resolution tropical channel model simulations of tropical cyclone climatology and intraseasonal-to-interannual variability. *Journal of Climate*, *32*(22), 7871–7895. https://doi.org/10.1175/JCLI-D-19-0130.1

Goldenberg, S. B., Landsea, C. W., Mestas-Nunez, A. M., & Gray, W. M. (2001). The recent increase in Atlantic hurricane activity: Causes and implications. *Science (New York, N.Y.)*, *293*(5529), 474–479. https://doi.org/10.1126/science.1060040

Haarsma, R., Acosta, M., Bakhshi, R., Bretonnière, P. A., Caron, L. P., Castrillo, M., et al. (2020). HighResMIP versions of EC-Earth: EC-Earth3P and EC-Earth3P-HR—Description, model computational performance and basic validation. *Geoscientific Model Development*, *13*(8), 3507–3527. https://doi.org/10.5194/gmd-13-3507-2020

Hodges, K., Cobb, A., & Vidale, P. L. (2017). How well are tropical cyclones represented in reanalysis datasets? *Journal of Climate*, *30*(14), 5243–5264. https://doi.org/10.1175/JCLI-D-16-0557.1

Hodges, K. I. (1995). Feature tracking on the unit sphere. *Monthly Weather Review*, *123*(12), 3458–3465. https://doi.org/10.1175/1520-0493(1995)123<3458:FTOTUS>2.0.CO;2

Hodges, K. I. (1999). Adaptive constraints for feature tracking. *Monthly Weather Review*, *127*(6), 1362–1373. https://doi.org/10.1175/1520-0493(1999)127

Hodson, D. L. R., Bretonnière, P. A., Cassou, C., Davini, P., Klingaman, N. P., Lohmann, K., et al. (2022). Coupled climate response to Atlantic Multidecadal Variability in a multi-model multi-resolution ensemble. *Climate Dynamics*, *59*(3), 805–836. https://doi.org/10.1007/S00382-022-06157-9

Huang, H., Patricola, C. M., & Collins, W. D. (2021). The influence of ocean coupling on simulated and projected tropical cyclone precipitation in the HighResMIP–PRIMAVERA simulations. *Geophysical Research Letters*, *48*(20), e2021GL094801. https://doi.org/10.1029/2021GL094801

Huang, H., Patricola, C. M., Winter, J. M., Osterberg, E. C., & Mankin, J. S. (2021). Rise in Northeast US extreme precipitation caused by Atlantic variability and climate change. *Weather and Climate Extremes*, *33*, 100351. https://doi.org/10.1016/J.WACE.2021.100351

Huang, H., Winter, J. M., & Osterberg, E. C. (2018). Mechanisms of abrupt extreme precipitation change over the northeastern United States. *Journal of Geophysical Research: Atmospheres*, *123*(14), 7179–7192. https://doi.org/10.1029/2017JD028136

Klotzbach, P. J., Bowen, S. G., Pielke, R., Bell, M., Klotzbach, P. J., Bowen, S. G., et al. (2018). Continental U.S. hurricane landfall frequency and associated damage: Observations and future risks. *Bulletin of the American Meteorological Society*, *99*(7), 1359–1376. https://doi.org/10.1175/BAMS-D-17-0184.1

Klotzbach, P. J., & Gray, W. M. (2008). Multidecadal variability in North Atlantic tropical cyclone activity. *Journal of Climate*, *21*(15), 3929–3935. https://doi.org/10.1175/2008JCLI2162.1

Knutson, T. R., Sirutis, J. J., Garner, S. T., Held, I. M., & Tuleya, R. E. (2007). Simulation of the recent multidecadal increase of Atlantic hurricane activity using an 18-km-grid regional model. *Bulletin of the American Meteorological Society*, *88*(10), 1549–1565. https://doi.org/10.1175/BAMS-88-10-1549

Kossin, J. P. (2018). A global slowdown of tropical-cyclone translation speed. *Nature*, *558*(7708), 104–107. https://doi.org/10.1038/s41586-018-0158-3

Kossin, J. P., Emanuel, K. A., & Vecchi, G. A. (2014). The poleward migration of the location of tropical cyclone maximum intensity. *Nature*, *509*(7500), 349–352. https://doi.org/10.1038/nature13278

Kreussler, P., Caron, L. P., Wild, S., Loosveldt Tomas, S., Chauvin, F., Moine, M. P., et al. (2021). Tropical cyclone integrated kinetic energy in an ensemble of HighResMIP simulations. *Geophysical Research Letters*, *48*(5), e2020GL090963. https://doi.org/10.1029/2020GL090963

Landsea, C. W., Pielke, R. A., Mestas-Nuñez, A. M., & Knaff, J. A. (1999). Atlantic basin hurricanes: Indices of climatic changes. *Climatic Change*, *42*(1), 89–129. https://doi.org/10.1023/A:1005416332322

Li, X., Xie, S. P., Gille, S. T., & Yoo, C. (2015). Atlantic-induced pan-tropical climate change over the past three decades. *Nature Climate Change*, *6*(3), 275–279. https://doi.org/10.1038/nclimate2840

Meehl, G. A., Hu, A., Castruccio, F., England, M. H., Bates, S. C., Danabasoglu, G., et al. (2020). Atlantic and Pacific tropics connected by mutually interactive decadal-timescale processes. *Nature Geoscience*, *14*(1), 36–42. https://doi.org/10.1038/s41561-020-00669-x

Murakami, H., Delworth, T. L., Cooke, W. F., Zhao, M., Xiang, B., & Hsu, P. C. (2020). Detected climatic change in global distribution of tropical cyclones. *Proceedings of the National Academy of Sciences of the United States of America*, *117*(20), 10706–10714. https://doi.org/10.1073/pnas.1922500117

O'Reilly, C., Patterson, M., Robson, J., Monerie, P., Hodson, D., & Ruprich-Robert, Y. (2022). Challenges with interpreting the impact of Atlantic Multidecadal Variability using SST-restoring experiments. https://doi.org/10.21203/rs.3.rs-1707393/v1

Patricola, C. M., Cassidy, D. J., & Klotzbach, P. J. (2022). Tropical oceanic influences on observed global tropical cyclone frequency. *Geophysical Research Letters*, *49*(13), e2022GL099354. https://doi.org/10.1029/2022GL099354

Patricola, C. M., Saravanan, R., & Chang, P. (2017). A teleconnection between Atlantic sea surface temperature and eastern and central North Pacific tropical cyclones. *Geophysical Research Letters*, *44*(2), 1167–1174. https://doi.org/10.1002/2016GL071965

Rappaport, E. N., & Blanchard, B. W. (2016). Fatalities in the United States indirectly associated with Atlantic tropical cyclones. *Bulletin of the American Meteorological Society*, *97*(7), 1139–1148. https://doi.org/10.1175/BAMS-D-15-00042.1

19448007, 2023, 10, Downloaded from https://agupubs.onlinelibrary.wiley.com/doi/10.1029/2023GL102959 by University Of East Anglia, Wiley Online Library on [20/07/2026]. See the Terms and Conditions (https://onlinelibrary.wiley.com/terms-and-conditions) on Wiley Online Library for rules of use; OA articles are governed by the applicable Creative Commons License

Roberts, M. J., Camp, J., Seddon, J., Vidale, P. L., Hodges, K., Vanniere, B., et al. (2020a). Impact of model resolution on tropical cyclone simulation using the HighResMIP-PRIMAVERA multimodel ensemble. *Journal of Climate*, *33*(7), 2557–2583. https://doi.org/10.1175/JCLI-D-19-0639.1

Roberts, M. J., Camp, J., Seddon, J., Vidale, P. L., Hodges, K., Vannière, B., et al. (2020b). Projected future changes in tropical cyclones using the CMIP6 HighResMIP multimodel ensemble. *Geophysical Research Letters*, *47*(14). https://doi.org/10.1029/2020GL088662

Ruprich-Robert, Y., Moreno-Chamarro, E., Levine, X., Bellucci, A., Cassou, C., Castruccio, F., et al. (2021). Impacts of Atlantic Multidecadal Variability on the tropical Pacific: A multi-model study. *Npj Climate and Atmospheric Science*, *4*(1), 1–11. https://doi.org/10.1038/s41612-021-00188-5

Ting, M., Camargo, S. J., Li, C., & Kushnir, Y. (2015). Natural and forced North Atlantic hurricane potential intensity change in CMIP5 models. *Journal of Climate*, *28*(10), 3926–3942. https://doi.org/10.1175/jcli-d-14-00520.1

U.S. Census Bureau. (2021). Emergency management coastal areas. Retrieved from https://www.census.gov/topics/preparedness/about/coastal-areas.html

Ullrich, P. A., Zarzycki, C. M., McClenny, E. E., Pinheiro, M. C., Stansfield, A. M., & Reed, K. A. (2021). TempestExtremes v2.1: A community framework for feature detection, tracking, and analysis in large datasets. *Geoscientific Model Development*, *14*(8), 5023–5048. https://doi.org/10.5194/GMD-14-5023-2021

Vecchi, G. A., & Knutson, T. R. (2008). On estimates of historical North Atlantic tropical cyclone activity. *Journal of Climate*, *21*(14), 3580–3600. https://doi.org/10.1175/2008JCLI2178.1

Voldoire, A., Saint-Martin, D., Sénési, S., Decharme, B., Alias, A., Chevallier, M., et al. (2019). Evaluation of CMIP6 DECK experiments with CNRM-CM6-1. *Journal of Advances in Modeling Earth Systems*, *11*(7), 2177–2213. https://doi.org/10.1029/2019MS001683

Wang, C., & Lee, S. K. (2009). Co-variability of tropical cyclones in the North Atlantic and the eastern North Pacific. *Geophysical Research Letters*, *36*(24), L24702. https://doi.org/10.1029/2009GL041469

Wang, C., Lee, S. K., & Enfield, D. B. (2008). Atlantic warm pool acting as a link between Atlantic multidecadal oscillation and Atlantic tropical cyclone activity. *Geochemistry, Geophysics, Geosystems*, *9*(5). https://doi.org/10.1029/2007GC001809

Webster, P. J., Holland, G. J., Curry, J. A., & Chang, H. R. (2005). Atmospheric science: Changes in tropical cyclone number, duration, and intensity in a warming environment. *Science*, *309*(5742), 1844–1846. https://doi.org/10.1126/SCIENCE.1116448/ASSET/EC277365-85DA-4321-B704-FE0F487B21F5/ASSETS/GRAPHIC/309_1844_F4.JPEG

Zhang, W., Vecchi, G. A., Murakami, H., Villarini, G., Delworth, T. L., Yang, X., & Jia, L. (2018). Dominant role of Atlantic multidecadal oscillation in the recent decadal changes in western North Pacific tropical cyclone activity. *Geophysical Research Letters*, *45*(1), 354–362. https://doi.org/10.1002/2017GL076397

19448007, 2023, 10, Downloaded from https://agupubs.onlinelibrary.wiley.com/doi/10.1029/2023GL102959 by University Of East Anglia, Wiley Online Library on [20/07/2026]. See the Terms and Conditions (https://onlinelibrary.wiley.com/terms-and-conditions) on Wiley Online Library for rules of use; OA articles are governed by the applicable Creative Commons License